

Joint Power Allocation and Antenna Placement for Pinching-Antenna Systems under User Location Uncertainty

Hao Feng, Ming Zeng, Xingwang Li, Wenwu Xie, Nian Xia and Octavia A. Dobre, Fellow, IEEE

Abstract—Pinching antenna systems have attracted much attention recently owing to its capability to maintain reliable line-of-sight (LoS) communication in high-frequency bands. By guiding signals through a waveguide and emitting them via a movable pinching antenna, these systems enable dynamic control of signal propagation and spatial adaptability. However, their performance heavily depends on effective resource allocation—encompassing power, bandwidth, and antenna positioning—which becomes challenging under imperfect channel state information (CSI) and user localization uncertainty. Existing studies largely assume perfect CSI or ideal user positioning, while our prior work considered uniform localization errors, an oversimplified assumption. In this paper, we develop a robust resource allocation framework for multi-user downlink pinching antenna systems under Gaussian-distributed localization uncertainty, which more accurately models real-world positioning errors. An energy efficiency (EE) maximization problem is formulated subject to probabilistic outage constraints, and an analytical power allocation strategy is derived under given antenna positions. On this basis, the heuristic particle swarm optimization (PSO) algorithm is employed to identify the antenna position that achieves the global EE configuration. Simulation results illustrate that the proposed scheme greatly enhances both EE and system reliability compared with fixed-antenna benchmark, validating its effectiveness for practical high-frequency wireless deployments.

I. Introduction

Pinching antenna systems have recently attracted considerable interest as a potential architecture for restoring line-of-sight (LoS) communication links in high-frequency regimes, including millimeter-wave (mmWave) and terahertz (THz) bands [1]–[6], and are therefore regarded as a key enabler for 6G and beyond networks. In such systems, user signals are first transmitted through a dielectric waveguide and subsequently radiated by a pinching antenna attached to it. By dynamically adjusting the antenna’s position along the waveguide, pinching antenna systems provide exceptional flexibility in controlling signal propagation, leading to improved spectral efficiency and adaptability [7]–[14].

H. Feng is with Hunan Institute of Engineering, Xiangtan, China, and also with Donghua University, Shanghai, China (e-mail: 1219001@mail.dhu.edu.cn).

M. Zeng is with Laval University, Quebec City, Canada (email: ming.zeng@gel.ulaval.ca).

X. Li is with Henan Polytechnic University, Jiaozuo, China (email: lixingwang@hpu.edu.cn).

W. Xie is with the School of Information Science and Engineering, Hunan Institute of Science and Technology, Yueyang, China (e-mail: gavinxie@hnist.edu.cn).

N. Xia is with Nanjing Normal University, Nanjing 210023, China. e-mail: nian.xia@nju.edu.cn

O. A. Dobre is with Memorial University, St. John’s, Canada (e-mail: odobre@mun.ca).

A core challenge in pinching-antenna systems is resource allocation, which involves the joint optimization of transmission parameters such as power, bandwidth, and antenna position to maximize system performance [15]. Most existing studies assume perfect channel state information (CSI) or accurate user location knowledge. However, in realistic deployments, channel estimation errors and localization inaccuracies are inevitable due to noise, hardware impairments, environmental dynamics, and pilot overhead limitations [16]. Ignoring such uncertainties can lead to substantial performance degradation, underscoring the necessity of robust resource allocation designs.

To the best of the authors’ knowledge, only two prior works have addressed robust resource allocation in pinching-antenna systems [17], [18]. In [17], a robust beamforming design is developed under imperfect CSI, where the actual channel is modeled as the superposition of an estimated component and an additive estimation error. However, the wireless channel component associated with the estimated CSI is assumed to be fixed and independent of the pinching-antenna position, which limits the practical applicability of the model, as the channel inherently depends on antenna placement. To overcome this limitation, [18] considers a joint robust power allocation and antenna position optimization framework under user location uncertainty. Nevertheless, the localization errors are modeled using a uniform distribution, which, although analytically convenient, does not accurately reflect the statistical characteristics of positioning errors encountered in practical systems. In contrast, Gaussian uncertainty models are widely recognized as providing a more realistic representation of the stochastic nature of localization errors [19], [20].

Motivated by these observations, this paper investigates robust resource allocation for pinching-antenna systems under Gaussian-distributed user localization uncertainty, with the objective of enhancing system reliability and energy efficiency (EE) in practical deployments. Specifically, we formulate an EE maximization problem for a multi-user downlink pinching-antenna system subject to user-specific probabilistic outage constraints. To tackle the resulting non-convex optimization problem with probabilistic constraints, we first derive an analytical power allocation solution for a fixed pinching-antenna position. Subsequently, the pinching-antenna position is optimized using a particle swarm optimization (PSO) algorithm to identify a globally energy-efficient configuration.

II. System Model and Problem Formulation

A. System Model

We examine a downlink multi-user scenario where an access point (AP), located at $(0, 0, 0)$ meters communicates with N single-antenna users with the aid of a pinching antenna mounted on a waveguide. The waveguide is placed following the x -axis, with a length of L meters and a height of d meters.

Denote the estimated location of user $n, n \in \{1, \dots, N\}$ as $\hat{\Phi}_n = (\hat{x}_n, \hat{y}_n, 0)$ meters. Unlike conventional studies assuming perfect location knowledge, we account for location uncertainty, that is, the true location of user n in the xy -plane $\Phi_n = (x_n, y_n)$ is modeled as a bivariate random vector following an isotropic normal distribution $(X_n, Y_n) \sim \mathcal{N}(\mu, \Sigma)$, where the mean vector is $\mu = (\hat{x}_n, \hat{y}_n)$, and the covariance matrix is $\Sigma = \sigma^2 \mathbf{I} = \begin{pmatrix} \sigma^2 & 0 \\ 0 & \sigma^2 \end{pmatrix}$. A higher variance value σ^2 means higher positioning error and vice versa. Note that the normal distribution has been widely adopted for positioning error [19], [20].

The users are scheduled using time-division multiple access (TDMA) to avoid mutual interference [4], [7]. To facilitate practical implementation of pinching antenna, it is assumed that the users share a common pinching antenna location [13], expressed as $\Phi^{\text{Pin}} = (x^{\text{Pin}}, 0, d)$ meters, where $x^{\text{Pin}} \in [0, L]$. Following the free-space propagation model, the achievable rate for user n in its assigned time slot is given by [4], [7]

$$R_n = \log_2 \left(1 + \frac{\eta P_n}{|\Phi_n - \Phi^{\text{Pin}}|^2 \sigma_n^2} \right). \quad (1)$$

Here, P_n is the transmit power for user n , while σ_n^2 represents the corresponding noise power. $\eta = \frac{c^2}{16\pi^2 f^2}$, c is the speed of light, and f is the carrier frequency [13].

Owing to positioning error in user locations, user n 's actual position Φ_n is modeled as a bivariate Gaussian random vector, which in turn makes the instantaneous achievable rate R_n a random variable. A transmission outage occurs whenever the instantaneous achievable rate R_n drops below a predefined target \hat{R}_n for user n . The outage probability is expressed as

$$\Pr \left[R_n < \hat{R}_n \mid \hat{\Phi}_n, \sigma^2 \right],$$

denoting the likelihood that R_n is less than the required target \hat{R}_n , conditioned over the estimated position $\hat{\Phi}_n$ and the error variance σ^2 . This metric characterizes the reliability of the AP—user n link under positioning error.

B. Problem Formulation

To ensure the quality of service (QoS), the outage probability for user $n, \forall n$ cannot exceed a maximum allowable threshold ε_n , i.e.,

$$\Pr \left[R_n < \hat{R}_n \mid \hat{\Phi}_n, \sigma^2 \right] \leq \varepsilon_n, \quad \forall n. \quad (2)$$

Under this constraint, we aim to maximize the system's EE, which is defined as the ratio of the effective sum rate, i.e., $\sum_{n=1}^N (1 - \varepsilon_n) \hat{R}_n$ [21] over the total transmit power, i.e., $\sum_{n=1}^N P_n$ [22], [23]. The problem is formulated as

$$\max_{x^{\text{Pin}}, P_n} \frac{\sum_{n=1}^N (1 - \varepsilon_n) \hat{R}_n}{\sum_{n=1}^N P_n} \quad (3a)$$

$$\text{s.t. } x^{\text{Pin}} \in [0, L], \quad (3b)$$

$$\Pr \left[R_n < \hat{R}_n \mid \hat{\Phi}_n, \sigma^2 \right] \leq \varepsilon_n, \quad \forall n, \quad (3c)$$

where (3b) limits the pinching antenna to the range of the waveguide, while (3c) constrains the outage probability by ε_n .

III. Proposed Solution

Since the parameters ε_n and \hat{R}_n are known, $\sum_{n=1}^N (1 - \varepsilon_n) \hat{R}_n$ is a constant. Therefore, the above EE maximization problem can be equivalently transformed into the following total power minimization problem:

$$\min_{x^{\text{Pin}}, P_n} \sum_{n=1}^N P_n \quad (4a)$$

$$\text{s.t. } x^{\text{Pin}} \in [0, L], \quad (4b)$$

$$\Pr \left[R_n < \hat{R}_n \mid \hat{\Phi}_n, \sigma^2 \right] \leq \varepsilon_n, \quad \forall n, \quad (4c)$$

In problem (4), both the objective function and constraint (4b) are linear. The major difficulty of solving it comes from the the probabilistic outage constraints in (4c), which are non-convex. Furthermore, the pinching antenna position enters the outage constraints of all users, thereby inducing coupling among these constraints. Consequently, they cannot be decoupled and must be addressed jointly, which significantly increases the overall problem complexity. To address problem (4), we first consider the case where the pinching antenna position is given. Based on the insight gained from this case, we will handle the pinching antenna position optimization in the end.

A. Power Optimization under given Pinching Antenna Position

Under given pinching antenna position, problem (4) becomes

$$\min_{P_n} \sum_{n=1}^N P_n \quad (5a)$$

$$\text{s.t. } \Pr \left[R_n < \hat{R}_n \mid \hat{\Phi}_n, \sigma^2 \right] \leq \varepsilon_n, \quad \forall n. \quad (5b)$$

Moreover, it is clear that minimizing the total transmit power equals to minimizing each user's transmit power individually, since the user powers are independent when the antenna position is fixed. Accordingly, Problem (5) can be equivalently transformed into N separate single-user power minimization subproblems as follows:

$$\min_{P_n} P_n \quad (6a)$$

$$\text{s.t. } \Pr \left[R_n < \hat{R}_n \mid \hat{\Phi}_n, \sigma^2 \right] \leq \varepsilon_n, \quad (6b)$$

We now examine constraint (6b) in greater detail. From (1), it follows that, for a given transmit power allocation P_n , the achievable rate R_n is solely a function of the Euclidean distance between the user and the pinching antenna. Consequently, all user locations lying on a sphere centered at the antenna experience an identical data rate, as shown in Fig. 1(a). For a prescribed target rate \hat{R}_n , we define R as the corresponding radius at which this rate is achieved, with R

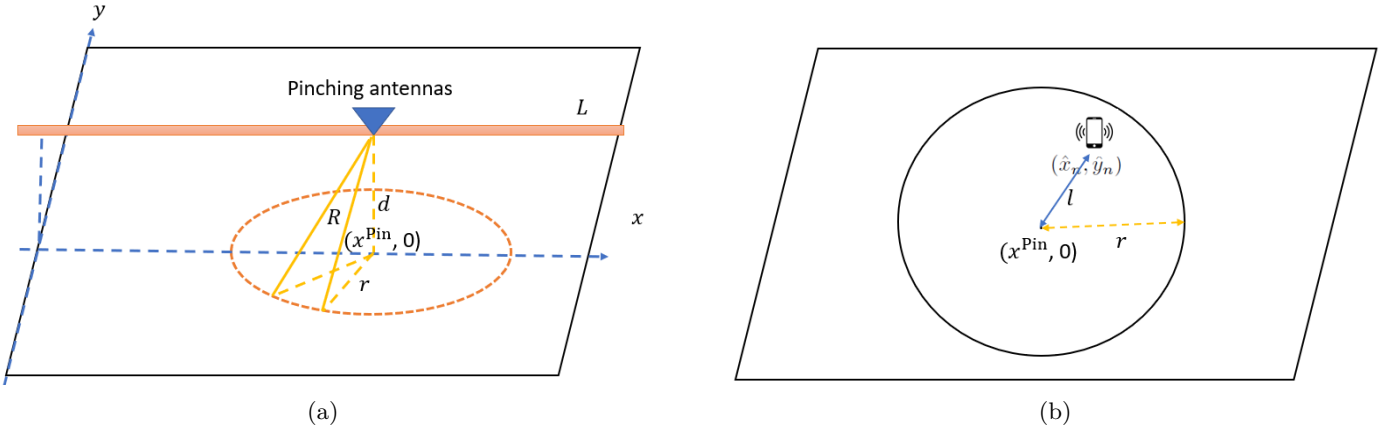


Fig. 1. Illustration of a) the antenna sphere achieving the target rate and its intersection with the user plane; and b) the user circle showing the center, the radius and the estimated user location.

to be determined. The intersection of this sphere with the user plane forms a circle centered at $(x^{\text{Pin}}, 0)$ with radius $r = \sqrt{R^2 - d^2}$, as shown in Fig. 1(b). Clearly, user locations within this circle yield a rate exceeding \hat{R}_n , and vice versa. As mentioned in the system model section, the true user location (X_n, Y_n) is a bivariate random vector following an isotropic normal distribution $(X_n, Y_n) \sim \mathcal{N}(\mu, \Sigma)$. To satisfy the outage probability ε_n , it means that the probability of the true user location lies within the circle centered at $(x^{\text{Pin}}, 0)$ with radius r should be at least $1 - \varepsilon_n$. Now the problem is how to calculate the probability that the true user location lies within the circle so that we can determine R . The following theorem gives the results.

Theorem 1. The probability of the true user location lies within the circle with radius r is given by

$$P((X_n - x^{\text{Pin}})^2 + Y_n^2 \leq r^2) = 1 - Q_1\left(\frac{l}{\sigma}, \frac{r}{\sigma}\right), \quad (7)$$

where $Q_1(a, b) = \int_b^\infty x e^{-\frac{x^2+a^2}{2}} I_0(ax) dx$ is the Marcum Q-function of order 1, with $I_0(\cdot)$ denoting the modified Bessel function of the first kind and order 0. Besides, $l = \sqrt{(\hat{x}_n - x^{\text{Pin}})^2 + \hat{y}_n^2}$ denotes the Euclidean distance between the projected antenna position on the user plane and the estimated location for user n .

Proof: Let us define two new random variables, W_1 and W_2 :

$$W_1 = \frac{X_n - x^{\text{Pin}}}{\sigma}$$

$$W_2 = \frac{Y_n}{\sigma}.$$

Since X_n and Y_n are independent normal variables, W_1 and W_2 are also independent normal variables with a unit variance:

$$W_1 \sim \mathcal{N}\left(\frac{\hat{x}_n - x^{\text{Pin}}}{\sigma}, 1\right)$$

$$W_2 \sim \mathcal{N}\left(\frac{\hat{y}_n}{\sigma}, 1\right).$$

The non-central chi-squared distribution with n degrees of freedom and non-centrality parameter λ is defined as the sum

of the squares of n independent normal random variables, each with unit variance.

Let us define a new variable $S = W_1^2 + W_2^2$. This variable, by definition, follows a non-central chi-squared distribution with:

- Degrees of freedom (n): $n = 2$, as there are two variables being summed.
- Non-centrality parameter (λ): λ is the sum of the squares of the means of W_1 and W_2 .

$$\lambda = \left(\frac{\hat{x}_n - x^{\text{Pin}}}{\sigma}\right)^2 + \left(\frac{\hat{y}_n}{\sigma}\right)^2 = \frac{(\hat{x}_n - x^{\text{Pin}})^2 + \hat{y}_n^2}{\sigma^2}. \quad (8)$$

With the Euclidean distance between the mean of the user location distribution and the center of the circle denoted by l , the non-centrality parameter is:

$$\lambda = \frac{l^2}{\sigma^2}. \quad (9)$$

The original probability statement can be rewritten in terms of our new variable S :

$$P((X_n - x^{\text{Pin}})^2 + Y_n^2 \leq r^2) = P(\sigma^2(W_1^2 + W_2^2) \leq r^2) \quad (10a)$$

$$= P(\sigma^2 S \leq r^2) \quad (10b)$$

$$= P\left(S \leq \frac{r^2}{\sigma^2}\right). \quad (10c)$$

This expression is the cumulative distribution function (CDF) of the non-central chi-squared distribution, evaluated at the point $\frac{r^2}{\sigma^2}$, and thus, is given by

$$P\left(S \leq \frac{r^2}{\sigma^2}\right) = F\left(\frac{r^2}{\sigma^2}; n = 2, \lambda = \frac{l^2}{\sigma^2}\right) \quad (11a)$$

$$= 1 - Q_1\left(\frac{l}{\sigma}, \frac{r}{\sigma}\right), \quad (11b)$$

where $F(\cdot)$ denotes the CDF of the non-central chi-squared distribution.

This concludes the proof, establishing that the probability is equivalent to the CDF of a non-central chi-squared distribution. The connection to the Marcum Q-function follows from the fact that the CDF of this specific non-central chi-squared distribution can be expressed in terms of the Marcum

Q-function [24]. Note that the calculation of the Marcum Q-function is embedded in numerical computing software, e.g., Matlab. \blacksquare

To satisfy the outage constraint, we have

$$1 - Q_1 \left(\frac{l}{\sigma}, \frac{r}{\sigma} \right) \geq 1 - \varepsilon_n \rightarrow Q_1 \left(\frac{l}{\sigma}, \frac{r}{\sigma} \right) \leq \varepsilon_n. \quad (12)$$

Clearly, $Q_1 \left(\frac{l}{\sigma}, \frac{r}{\sigma} \right)$ declines with r . Therefore, there exists a minimum r such that equality is obtained for (12). Denote this minimum value of r by r_{\min} , that is, $Q_1 \left(\frac{l}{\sigma}, \frac{r_{\min}}{\sigma} \right) = \varepsilon_n$. Note that r_{\min} can be easily obtained using the bisection method by exploiting the monotonicity of the function $Q_1 \left(\frac{l}{\sigma}, \frac{r}{\sigma} \right)$ over r .

To meet the QoS constraint, when $r = r_{\min}$, we should have $R_n \geq \hat{R}_n$. That is,

$$\log_2 \left(1 + \frac{\eta P_n}{|\Phi_n - \Phi^{\text{Pin}}|^2 \sigma_n^2} \right) \geq \hat{R}_n \quad (13a)$$

$$\rightarrow \log_2 \left(1 + \frac{\eta P_n}{(r_{\min}^2 + d^2) \sigma_n^2} \right) \geq \hat{R}_n \quad (13b)$$

$$\rightarrow P_n \geq \frac{(2^{\hat{R}_n} - 1)(r_{\min}^2 + d^2) \sigma_n^2}{\eta}. \quad (13c)$$

Accordingly, we have the minimum power that satisfies the outage probability constraint for user n given by

$$P_n^{\min} = \frac{(2^{\hat{R}_n} - 1)(r_{\min}^2 + d^2) \sigma_n^2}{\eta}. \quad (14)$$

B. Pinching Antenna Position Optimization

With the relation between the power and radius given by (14), it is time to consider the pinching antenna position optimization. For user n , optimizing the pinching antenna means adjusting the value of x^{Pin} . This will directly affect the value of l in the Marcum Q-function. Based on the characteristic of the Marcum Q-function, to obtain the outage probability ε_n , r_{\min} grows with l and vice versa. Since a smaller value of r_{\min} is preferred based on (14), a smaller value of l is preferred as well. According to the definition of l , minimizing l means placing the pinching antenna as close as possible to the estimated user location. This is consistent with systems with perfect user location information. However, as in the systems with perfect user location information, obtaining the optimal pinching antenna under multi-user setup is non-trivial because of the competitive nature of the users [11]. The dependence of each user's minimum required transmit power on the antenna position is dictated by the outage probability constraint. As discussed earlier, this dependence does not admit a closed-form representation and is non-differentiable because it is obtained via a bisection procedure. Consequently, standard gradient-based optimization techniques are not applicable.

To overcome this limitation, we employ a heuristic PSO approach, which operates without the need for derivative information. The PSO implementation follows well-established procedures and is readily supported by platforms such as MATLAB; therefore, the algorithmic details are omitted for brevity. The central task lies in evaluating the objective function—namely, the minimum total transmit power—which

is computed by applying the previously developed solution for a given pinching antenna location.

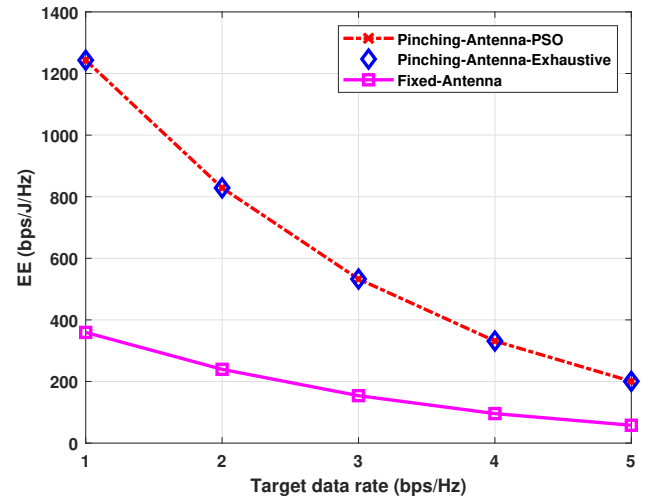


Fig. 2. EE versus target data rate at the users.

IV. Numerical Results

Here we report numerical simulations conducted to assess the effectiveness of the proposed pinching-antenna-based transmission framework. Unless otherwise specified, the simulation setup considers a system serving $N = 5$ users, whose estimated locations are independently and uniformly distributed within a rectangular region of dimensions $120 \text{ m} \times 20 \text{ m}$. The variance of the user location distribution is set to $\sigma^2 = 1$. The target spectral efficiency for each user is fixed at $\hat{R}_n = 3 \text{ bps/Hz}$, while the maximum tolerable outage probability is $\varepsilon_n = 0.01, \forall n$. The system operates at a carrier frequency of 28 GHz with an aggregate bandwidth of 100 MHz, and the noise power is assumed to be -94 dBm . The waveguide is characterized by a length of $L = 50 \text{ m}$ and a vertical height of $d = 3 \text{ m}$. All numerical results are obtained by averaging over 100 random Monte Carlo trials.

For benchmarking purposes, two reference schemes are adopted:

- **Exhaustive search:** This scheme determines the optimal pinching-antenna location by conducting a one-dimensional exhaustive search along the waveguide.
- **Fixed-antenna architecture:** In this scheme, the antenna remains fixed at the position $(0, 0, d) \text{ m}$, representing a conventional static antenna configuration.

Figure 2 plots the EE versus the users' target data rate for all considered schemes. It is observed that the EE monotonically decreases with increasing target data rate across all configurations. This behavior can be attributed to the definition of EE as the ratio between the effective sum rate and the total transmit power. For a fixed outage probability constraint, the effective sum rate scales linearly with the target data rate, whereas the required transmit power grows exponentially with the target data rate, as indicated by (14). As a result, the EE degrades as the target data rate increases. Furthermore, for the entire range of target data rates, the pinching-antenna-based schemes substantially outperform the fixed-antenna architecture, highlighting the performance advantage

enabled by antenna mobility. In addition, the proposed PSO-based algorithm achieves performance nearly identical to that of the exhaustive-search benchmark, thereby confirming its near-optimality.

Figure 3 depicts the EE versus the outage probability constraint ε_n for all considered schemes. For a fixed target data rate, the effective sum rate decreases linearly with the outage probability constraint ε_n . Meanwhile, from (12) and noting that the Marcum Q -function $Q_1\left(\frac{L}{\sigma}, \frac{r}{\sigma}\right)$ is monotonically decreasing with respect to r , a larger ε_n corresponds to a smaller minimum distance requirement r_{\min} . According to (14), this relaxation leads to a reduction in the required total transmit power as ε_n increases. The mildly decreasing trend observed for all curves in Fig. 3 indicates that the reduction in total transmit power is slightly less pronounced than the corresponding decrease in the effective sum rate, resulting in a net decline in EE. Once again, the pinching-antenna-based schemes consistently outperform the fixed-antenna architecture, demonstrating the performance gains enabled by antenna mobility.

Finally, Fig. 4 shows how the EE varies with the standard deviation of the user location uncertainty, denoted by σ . It is found that the effective sum rate remains invariant with respect to σ , since both the target data rate and the outage probability constraint are fixed. In contrast, to satisfy the prescribed QoS requirements under increased location uncertainty, the minimum required distance r_{\min} increases monotonically with σ , which in turn leads to a higher total transmit power according to (14). As a result, the EE decreases with σ for all above considered schemes. Moreover, the degradation in EE is more pronounced for the pinching-antenna-based schemes than for the fixed-antenna architecture. Such a behavior can be attributed to the fact that a larger variance σ^2 implies greater spatial uncertainty, thereby diminishing the effectiveness of antenna position optimization. Nevertheless, within the considered range of location variance, the pinching-antenna-based schemes consistently achieve significantly higher EE compared to the fixed-antenna benchmark.

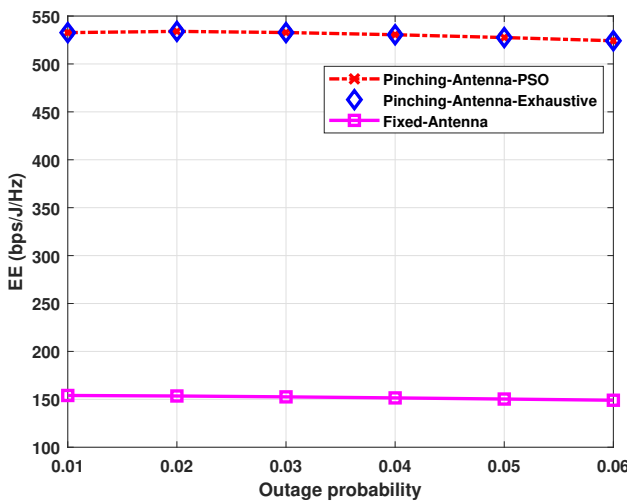


Fig. 3. EE versus users' outage probability ε_n .

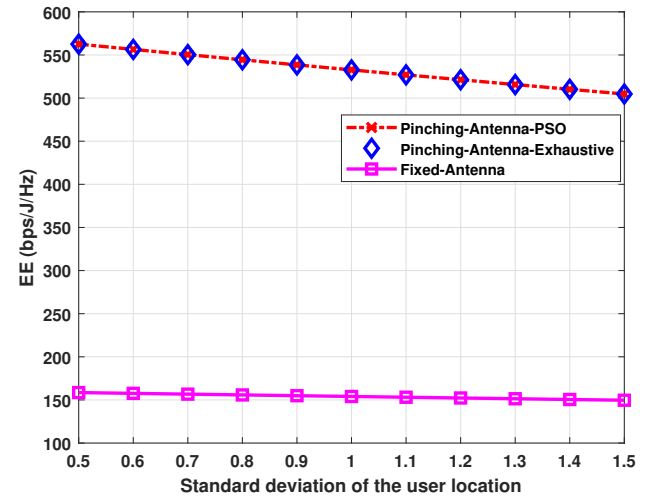


Fig. 4. EE versus the standard deviation of the user locations.

V. Conclusion

In this paper, we studied a robust joint optimization framework for transmit power allocation and pinching-antenna placement in downlink pinching-antenna systems under Gaussian-distributed user localization uncertainty. The goal was to maximize the EE of multi-user downlink transmissions while satisfying probabilistic outage constraints. The first-order Marcum Q -function was utilized to accurately model the statistical distribution of the users' actual locations, enabling the derivation of the minimum transmit power required to meet each user's outage probability requirement. The optimal pinching-antenna position was subsequently obtained using an efficient PSO algorithm. Numerical results show that the proposed pinching-antenna-based schemes consistently and significantly outperform the conventional fixed-antenna architecture in terms of EE, and that the PSO-based solution achieves near-optimal performance compared with the exhaustive-search benchmark.

References

- [1] A. Fukuda et al., "Pinching antenna using a dielectric waveguide as an antenna," Technical Journal, vol. 23, no. 3, pp. 5–12, Jan. 2022.
- [2] Z. Yang et al., "Pinching antennas: Principles, applications and challenges," IEEE Wirel. Commun., pp. 1–10, 2025.
- [3] K. R. Wijewardhana et al., "Wireless-fed pinching-antenna systems (wi-pass) for nextg wireless networks," 2025. [Online]. Available: <https://arxiv.org/abs/2510.18743>
- [4] Z. Ding, R. Schober, and H. Vincent Poor, "Flexible-antenna systems: A pinching-antenna perspective," IEEE Trans. Commun., vol. 73, no. 10, pp. 9236–9253, Oct. 2025.
- [5] J. Zhao, X. Mu, K. Cai, Y. Zhu, and Y. Liu, "Waveguide division multiple access for pinching-antenna systems (PASS)," arXiv: 2502.17781, 2025.
- [6] J. Xiao et al., "Frequency-selective modeling and analysis for OFDM-integrated wideband pinching-antenna systems," IEEE Wirel. Commun. Lett., vol. 14, no. 11, pp. 3500–3504, Nov. 2025.
- [7] X. Xie et al., "A low-complexity placement design of pinching-antenna systems," IEEE Commun. Lett., vol. 29, no. 8, pp. 1784–1788, Aug. 2025.
- [8] K. Wang et al., "Antenna activation for NOMA assisted pinching-antenna systems," IEEE Wirel. Commun. Lett., vol. 14, no. 5, pp. 1526–1530, May 2025.

[9] S. Hu, R. Zhao, Y. Liao, D. W. K. Ng, and J. Yuan, "Sum-rate maximization for pinching antenna-assisted NOMA systems with multiple dielectric waveguides," 2025. [Online]. Available: <https://arxiv.org/abs/2503.10060>

[10] Y. Li et al., "Pinching antenna-aided wireless powered communication networks," *IEEE Wirel. Commun. Lett.*, vol. 15, pp. 255–259, 2026.

[11] M. Zeng et al., "Sum rate maximization for NOMA-assisted uplink pinching-antenna systems," *IEEE Wirel. Commun. Lett.*, vol. 15, pp. 280–284, 2026.

[12] Y. Fu, F. He, Z. Shi, and H. Zhang, "Power minimization for noma-assisted pinching antenna systems with multiple waveguides," 2025. [Online]. Available: <https://arxiv.org/abs/2503.20336>

[13] S. A. Tegos, P. D. Diamantoulakis, Z. Ding, and G. K. Karagiannidis, "Minimum data rate maximization for uplink pinching-antenna systems," *IEEE Wirel. Commun. Lett.*, vol. 14, no. 5, pp. 1516–1520, May 2025.

[14] J. Zhao, H. Song, X. Mu, K. Cai, Y. Zhu, and Y. Liu, "Pinching-antenna systems-enabled multi-user communications: Transmission structures and beamforming optimization," *IEEE Trans. Commun.*, pp. 1–1, 2025.

[15] M. Zeng, J. Wang, O. A. Dobre, Z. Ding, G. K. Karagiannidis, R. Schober, and H. V. Poor, "Resource allocation for pinching-antenna systems: State-of-the-art, key techniques and open issues," 2025. [Online]. Available: <https://arxiv.org/abs/2506.06156>

[16] J. Xiao, J. Wang, and Y. Liu, "Channel estimation for pinching-antenna systems (PASS)," *IEEE Commun. Lett.*, vol. 29, no. 8, pp. 1789–1793, Aug. 2025.

[17] M. Sun, C. Ouyang, S. Wu, and Y. Liu, "Robust beamforming for pinching-antenna systems," *IEEE Trans. Veh. Tech.*, pp. 1–6, 2026.

[18] M. Zeng, X. Wang, Y. Liu, Z. Ding, G. K. Karagiannidis, and H. V. Poor, "Robust resource allocation for pinching-antenna systems under user location uncertainty," *IEEE Trans. Veh. Tech.*, pp. 1–5, 2026.

[19] B. Hofmann-Wellenhof, K. Legat, and M. Wieser, *Navigation: principles of positioning and guidance*. Springer Science & Business Media, 2011.

[20] S. Mertikas et al., "Error distribution and accuracy measure in navigation: An overview," 2023.

[21] F. Fang, K. Wang, Z. Ding, and V. C. M. Leung, "Energy-efficient resource allocation for NOMA-MEC networks with imperfect CSI," *IEEE Trans. Commun.*, vol. 69, no. 5, pp. 3436–3449, May 2021.

[22] Y. Zhang, H.-M. Wang, T.-X. Zheng, and Q. Yang, "Energy-efficient transmission design in non-orthogonal multiple access," *IEEE Trans. Veh. Tech.*, vol. 66, no. 3, pp. 2852–2857, Mar. 2017.

[23] M. Zeng, N.-P. Nguyen, O. A. Dobre, Z. Ding, and H. V. Poor, "Spectral- and energy-efficient resource allocation for multi-carrier uplink NOMA systems," *IEEE Trans. Veh. Tech.*, vol. 68, no. 9, pp. 9293–9296, Mar. 2019.

[24] M. K. Simon, *Probability Distributions Involving Gaussian Random Variables*. Springer, 2002.